Available online at www.sciencedirect.com
SCIENCE DIRECT®
Journal of Sound and Vibration 271 (2004) 323–337
JOURNAL OF SOUND AND VIBRATION
www.elsevier.com/locate/jsvi

Active vibration isolation of a flexible structure mounted on a vibrating elastic base

A.H. El-Sinawi*

Department of Mechanical Engineering, King Fahd University of Petroleum and Minerals, KFUPM P.O. Box 1887, Dhahran 31261, Saudi Arabia

Received 14 November 2001; accepted 24 February 2003

Abstract

The problem of isolating the vibration at any location on a flexible structure mounted on a vibrating flexible base is considered using a Kalman-based active feedforward–feedback controller (KAFB) with non-collocated sensors and actuators. The control strategy developed in this study focuses on lowering the force transmitted to the structure through its vibrating elastic foundation in the presence of process and measurements noise. A state-space model of the structure is constructed from the natural frequencies and mode shapes generated via finite element modal analysis of the structure. The important aspect of the proposed control strategy is that, while it's design is based on a full order model of the physical structure (plant), its implementation is reduced to the realization of a second order estimator regardless of the order of the plant model, and with negligible effect on its accuracy and performance. Therefore, the proposed control strategy requires low computational effort, which makes it well suited for real time control applications. Another unique aspect of this control strategy is its agility and speed in compensating for any phase or magnitude mismatch between transmitted force and control force. Moreover, the stability of the control system is implicitly attained by the controllability condition posed by the Kalman filter on the model. Thus, proper choice of Kalman gains will drive the states of the structure, at the sensor location, ideally to zero. In addition to that, digital implementation of the proposed controller can be easily done considering the fact that the discrete Kalman filter is exact. Numerical simulation of the controller performance is carried out and the results are presented.

1. Introduction

The control of vibration transmission has received much attention in recent years due to its effect on the functionality of systems involved. For example, vibration transmitted from the

*Tel.: +966-3-860-2455; fax: +966-3-860-2949.
E-mail address: elsinawi@kfupm.edu.sa (A.H. El-Sinawi).

0022-460X/$ - see front matter © 2003 Published by Elsevier Ltd.
doi:10.1016/S0022-460X(03)00771-5

engine of an automobile to its chassis causes unwanted noise and discomfort to the passengers. Vibration transmission in precision machining and precision positioning systems degrades its precision. In other applications, vibration transmission can cause instability [1] or even failure, as is the case in buildings subject to earthquakes, or sensitive avionics mounted on the airframe of an aircraft. The wide spectrum of problems caused by vibration transmission has generated interest in the field of control and isolation of vibration transmission [2].

In general, the purpose of vibration transmission control is to isolate the environment from the source vibration by lowering the transmitted force between the two. Depending on the application, the source of vibration can be the base or the structure itself [3]. A good vibration isolator is potentially a poor shock isolator. Adding damping to decrease transmissibility near resonance (frequency ratio $<1/\sqrt{2}$) increases the transmissibility at isolation frequencies (frequency ratio $>1/\sqrt{2}$). To complicate matters, isolation design is limited by the elastic deflection and the rattle space of the isolation device [4]. For passive dampers, elastomeric isolators are the most commonly used passive devices for vibration isolation. The stiffness required of such mounts for supporting elastic loads, e.g., weight of the structure, could lead to limitation in their isolation capabilities. In addition, the damping requirements of the mount at low and high frequency ranges are different, since large damping is needed for low frequency isolation and low damping is needed for high frequency isolation. For this reason, tuned isolators such as hydraulic mounts have been developed to remedy this contradiction in damping requirements [5]. These tuned isolators are passive vibration isolation mechanisms that are tuned to a certain resonant frequency and only add damping to that resonance; however, once they are tuned they are not adaptable.

Vibration damping (for shock isolation) and vibration cancellation (for vibration isolation) can be accommodated by active control. The advantage of using active control techniques over its passive counterparts is their capability to adapt to changes in the natural frequency of the system and/or excitation frequencies. Kaplow and Velman [6] isolated two structures by using active mounts to apply force between the structure and its vibrating base based on acceleration measurements. Their idea was to maintain zero acceleration of the isolated side. Gardonio et al. [7,8] presented and analyzed five different techniques for active isolation of structural vibration on a multi degree of freedom system. The system in their study consisted of a rigid mass acting as a vibration source, connected to a receiver plate through a pair of mounts each of which can generate axial control force. They concluded that controlling the total power transmitted to the plate gives best results under ideal conditions. However, they suggested that for the realistic cases, the cancellation of velocity or forces is more effective than the control of measured power. For a comprehensive literature survey on vibration isolation see Refs. [1,7,8].

A common vibration cancellation technique is the feedforward control. Ideally, such a technique should cause complete cancellation of the disturbance effect at the sensor location assuming that (a) the overall gain of the controller and error path matches the forward path gain exactly and (b) the combined controller and error path is exactly 180° out of phase with the forward path. When these parameters are not met, the cancellation could actually deteriorate the system disturbance response.

Considering the importance of gain and phase matching in feedforward control, it is desirable to implement some type of adaptive algorithm to minimize these errors. Least mean square

algorithms, based on minimizing the mean square of the disturbance response are commonly used in noise and vibration control [9,10].

In many cases successful implementation of active vibration control depends on, among other things, the accuracy of the model of the system to be controlled. In large flexible structures and due to the complexity of equation of motion, discretization is frequently used for constructing a finite-dimensional system of ordinary differential equations [11]. However, reducing the infinite-dimensional distributed system to a finite-dimensional system (discretized) causes some problems such as spillover, sensitivity to small parameter perturbation, as well as uncertainties [11,12]. Moreover, another problem that arises from discretization is that many modes may need to be considered, especially if it is desired to control the vibration of large flexible structures over a wide range of frequencies [13].

In this paper, the problem of isolating the vibration of any location on a flexible structure from the vibration of its elastic base is considered using a Kalman-based active feedforward–feedback controller with non-collocated sensor and actuator. The control strategy developed in this study focuses on lowering the force transmitted to the structure through its vibrating elastic foundation in the presence of process and measurements noise. A state-space mode of the structure is constructed from the natural frequencies and mode shapes generated via finite element modal analysis of the structure. The important aspect of the proposed control strategy is that, while it's design is based on a full order model of the physical structure (plant), its implementation is reduced to the realization of a second order estimator regardless of the order of the plant model, and with negligible effect on its accuracy and performance. Therefore, the proposed controller strategy requires low computational effort, which makes it well suited for inline control applications. Another unique aspect of this control strategy is its agility and speed in compensating for any phase or magnitude mismatch between transmitted force and control force. Moreover, the stability of the control system is implicitly attained by the controllability condition posed by the Kalman filter on the model. Thus, proper choice of the Kalman gains will drive the states of the structure at the sensor location to zero as required. In addition to that, digital implementation of the proposed controller can be easily done considering the fact that the discrete Kalman filter is exact. Numerical simulation of the controller performance is carried out and the results are presented.

Knowing that the model upon which the Kalman estimator is constructed in this study can always be reduced to second order, and always resembles that of the actual system, the speed and agility required for compensating for any phase or magnitude mismatch between the transmitted force and the control force is almost instant. Such high performance is accredited to the low order of the estimator and, unlike feedforward controllers, the feedforward–feedback approach also monitors the output of the system. In this case, any output deviation from the expected value (zero acceleration) at the sensor location is compensated for by adjusting the magnitude and the phase of the control force to achieve the desired zero acceleration.

2. Finite element model

To implement the proposed scheme on a distributed parameter system such as the beam shown in Fig. 1, the structure is discretized into finite elements forming an n-dimensional discrete spring–

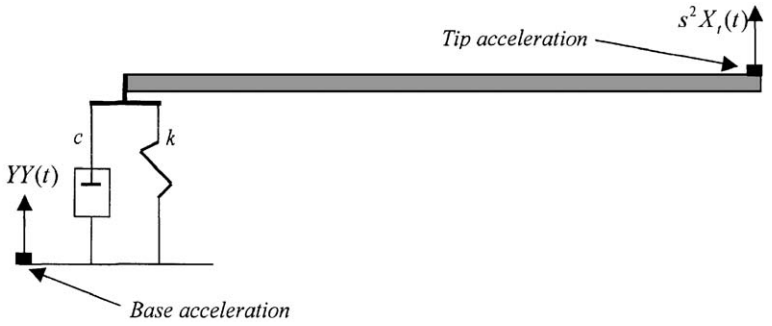

Fig. 1. Flexible beam mounted on a vibrating elastic base.

mass–damper system whose dynamics is described by the second order matrix differential equation,

$$\mathbf{M}\ddot{\mathbf{x}} + \mathbf{C}\dot{\mathbf{x}} + \mathbf{K}\mathbf{x} = \mathbf{u}(t), \tag{1}$$

where **M**, **C**, and **K** are the $(n \times n)$ square and symmetric mass, damping, and stiffness coefficient matrices respectively. The variables $\mathbf{x}(t)$ and $\mathbf{u}(t)$ are the displacement and force vectors, respectively. For systems with proportional damping, the matrices **M**, **K**, and **C** can be diagonalized using normalized orthonormal eigenvectors as the columns of the transformation matrix [1,12], yielding

$$\ddot{\eta}_i(t) + 2\varsigma_i\omega_i\eta_i(t) + \omega_i\eta_i(t) = V_i u(t), \quad i = 1, \ldots, n, \tag{2}$$

where η_i, ω_i, and ς_i represent the transformed co-ordinates, natural frequency, and damping ratio of the structure's ith mode of vibration, respectively. When the input is point force (i.e., actuators), V_i is the vector of the ith mode shape evaluated at the force input location.

For flexible structures having point force(s) as the input(s) and point displacement(s) as the measured output, the state-space model of flexible structures can be constructed in the form,

$$\dot{\mathbf{z}} = \begin{bmatrix} \mathbf{0} & \mathbf{I} \\ -\mathbf{\Omega}^2 & -2\varsigma\mathbf{\Omega} \end{bmatrix}\mathbf{z} + \begin{bmatrix} \mathbf{0} \\ \mathbf{V} \end{bmatrix}\mathbf{u}, \tag{3}$$

$$\mathbf{X}_t = [\mathbf{W}\ \ \mathbf{0}]\mathbf{z} + \mathbf{D}\mathbf{u}, \tag{4}$$

where, state vector:

$$\mathbf{z}(t) = \begin{Bmatrix} \boldsymbol{\eta}(t) \\ \dot{\boldsymbol{\eta}}(t) \end{Bmatrix},$$

number of modes:

$$N_m,$$

number of inputs:

$$N_u,$$

number of outputs:

$$N_y,$$

modal displacement:

$$\boldsymbol{\eta}(t) = \{\eta_1(t), \eta_2(t), \ldots, \eta_{N_m}(t)\}^{\mathrm{T}},$$

modal velocity:

$$\dot{\boldsymbol{\eta}}(t) = \{\dot{\eta}_1(t), \dot{\eta}_2(t), \ldots, \dot{\eta}_{N_m}(t)\}^{\mathrm{T}},$$

input:

$$\mathbf{u}(t) = \{u_1(t), u_2(t), \ldots, u_{N_u}(t)\}^{\mathrm{T}},$$

output matrix

$$\mathbf{W} = \begin{bmatrix} \psi_{1,1}, & \cdots\cdots, & \psi_{N_m,1} \\ \vdots & \ddots & \vdots \\ \psi_{1,N_y}, & \cdots\cdots, & \psi_{N_m,N_y} \end{bmatrix}.$$

The state-space model of Eqs. (3) and (4) can be expressed in the following compact form:

$$\dot{z} = \mathbf{A}_s(\theta)z + \mathbf{B}_s(\theta)u, \tag{5}$$

$$y = \mathbf{C}_s(\theta)z + \mathbf{D}_s(\theta)u, \tag{6}$$

where $\mathbf{A}_s, \mathbf{B}_s, \mathbf{C}_s$, and $\mathbf{D}_s$ matrices are functions of the system (natural frequency, damping ratio, and mode shapes (i.e., if we assume $\theta = f(\omega_i, \zeta_i,$ and $\psi_i)_{i=1,\ldots,n}$).

The information needed to construct the matrices $\mathbf{A}_s$, $\mathbf{B}_s$, $\mathbf{C}_s$, and $\mathbf{D}_s$ of Eqs. (5) and (6) (i.e., mode shapes and natural frequencies) can be obtained by performing FE modal analysis of the solid model of the plant.

3. Controller design

Assuming that the control effort will be used for the purpose of isolating the tip of the beam shown in Fig. 1 from the vibration of the elastic base and to better explain the proposed control strategy, consider a single degree-of-freedom spring–mass–damper system mounted on a vibrating elastic base. Such system has the equation of motion:

$$m\ddot{x} + c\dot{x} + kx = c\dot{y} + ky, \tag{7}$$

where c and k are the elastic base damping and stiffness, respectively. The variable x is the physical displacement of the mass m and y is the physical displacement of the base (i.e., disturbance). The Laplace transform of Eq. (7) is

$$(ms^2 + cs + k)X(s) = (cs + k)Y(s) \tag{8}$$

and the transfer function mapping the base displacement to that of the mass is

$$G(s) = \frac{X(s)}{Y(s)} = \frac{(cs + k)}{(ms^2 + cs + k)}. \tag{9}$$

Considering that accelerometers are the sensors of choice in most vibration measurements and control applications, the transfer function of Eq. (9) can be modified in such a way that the acceleration of the base is the input to the beam's structure and the acceleration of any point on the beam (where vibration isolation is desired) is the system's output. Thus, the modified transfer function takes on the form,

$$G(s) = \frac{s^2 X(s)}{s^2 Y(s)} = \frac{(cs+k)}{s^2} \cdot \frac{s^2}{(ms^2+cs+k)}, \tag{10}$$

where $(s^2 Y)$ is the acceleration of the base and $(s^2 X)$ is the acceleration of the mass. According to Eq. (10), the block diagram of the physical system can be represented as shown in Fig. 2 which has

$$G_f(s) = \frac{(cs+k)}{s^2}, \tag{11}$$

and

$$G_s(s) = \frac{s^2}{(ms^2+cs+k)}. \tag{12}$$

It is clear that by having the base acceleration as the input to the first block (i.e., $G_f(s)$) of Fig. 2, the transfer function of that block becomes proper, rational and thus, realizable.

Notice that the double integrator in the denominator of the block $G_f(s)$ can make the realization unstable unless the correct initial conditions are used. Since the initial conditions are not known in active vibration isolation applications, a second order filter that has a natural frequency well below the disturbance frequency(s) approximates the double integrator. Moreover, replacing the double integrator by a second order filter eliminates the possibility of saturating the integrator by DC offset of the accelerometer and the associated electronics. By doing so, the block representing $G_f(s)$, (also referred to as the transmitted force block) is approximated as

$$G_f(s) = \frac{\omega_f(cs+k)}{(s^2+2\varsigma_f\omega_f s+\omega_f^2)}, \tag{13}$$

where ω_f, and ς_f are the natural frequency and the damping ratio of the filter, respectively. The second order filter behaves as an integrator in the frequency range R, where $\omega_f \leqslant R \leqslant 2\pi k/c$ [14].

The (KAFB) dynamic model is formed from the combined dynamics of the transmitted force $G_f(s)$ of Eq. (13) and the dynamics of the structure $G_s(s)$ of Eq. (12).

The equivalent continuous state-space model of the transmitted force $G_f(s)$ is

$$\dot{x}_f = \mathbf{A}_f \mathbf{x}_f + \mathbf{B}_f \mathbf{YY},$$

$$\mathbf{F} = \mathbf{C}_f \mathbf{x}_f + \mathbf{D}_f \mathbf{YY}, \tag{14}$$

where $(\mathbf{YY}(t))$ is the base acceleration, $\mathbf{x}_f$ is a vector of the transmitted force states. $\mathbf{A}_f$, $\mathbf{B}_f$, $\mathbf{C}_f$, and $\mathbf{D}_f$, are dynamics, input, output, and direct input matrices of the transmitted force block of Fig. 2,

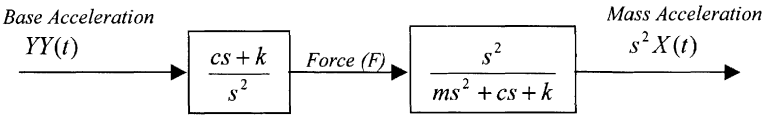

Fig. 2. Block diagram of a spring–mass–damper system subject to base excitation.

respectively. The term **F** denotes the force transmitted to the mass m through its elastic base and is a function of time.

Using the above analysis and replacing the mass m with the beam of Fig. 1, one can express the continuous state-space model of the structure depicted by Eqs. (6) and (7) as

$$\dot{\mathbf{z}}_f = \mathbf{A}_s\mathbf{z} + \mathbf{B}_s\mathbf{F},$$

$$\mathbf{X}_t = \mathbf{C}_s\mathbf{z} + \mathbf{D}_s\mathbf{F}, \tag{15}$$

where that the term $u(t)$ of Eqs. (5) and (6) has been replaced by **F** in Eq. (15) to indicate that the input to the structure is the force transmitted to it through its elastic base.

A state-space model of the beam-base system (the transmitted force represented by Eq. (14) and the structure represented by Eq. (15)) can now be constructed by augmenting the two parts together [14] such that

$$\mathbf{A}_a = \begin{bmatrix} \mathbf{A}_f & \mathbf{0} \\ \mathbf{B}_s\mathbf{C}_f & \mathbf{A}_s \end{bmatrix}, \tag{16}$$

$$\mathbf{B}_a = \begin{bmatrix} \mathbf{B}_f \\ \mathbf{B}_s\mathbf{D}_f \end{bmatrix}, \tag{17}$$

$$\mathbf{C}_a = [\mathbf{D}_s\mathbf{C}_f \;\; \mathbf{C}_s], \tag{18}$$

$$\mathbf{D}_a = [\mathbf{D}_f\mathbf{D}_s], \tag{19}$$

where $\mathbf{A}_a$, $\mathbf{B}_a$, $\mathbf{C}_a$, $\mathbf{D}_a$ represent the state-space matrices of the augmented base-beam system in which, the first two states belong to the transmitted force part and the remaining states belong to the structure mounted on the base.

Matrices $\mathbf{A}_a$, $\mathbf{B}_a$, and $\mathbf{C}_a$ are used for designing the (KAFB) matrix of gains ($\mathbf{K}_a$) such that

$$\mathbf{K}_a = \mathbf{S}_o\mathbf{C}_a^{\mathrm{T}}\mathbf{R}^{-1}. \tag{20}$$

The column vector $\mathbf{K}_a$ in this case is a $(2+2n)\times 1$ column vector, and the first two rows are the Kalman gains of the states of the transmitted force, and the remaining $2n$ gains are those of the states of the structure. $\mathbf{S}_o$ is the steady state solution of the following filter algebraic *Riccati* equation,

$$\dot{\mathbf{S}} = \mathbf{A}_a\mathbf{S} + \mathbf{S}\mathbf{A}^{\mathrm{T}} - \mathbf{S}\mathbf{C}_a^{\mathrm{T}}\mathbf{R}^{-1}\mathbf{C}_a\mathbf{S} + \mathbf{B}_a\mathbf{Q}\mathbf{B}_a^{\mathrm{T}}. \tag{21}$$

Matrices **R** and **Q** positive definite and positive semi-definite matrices, respectively [15]. For a specific value of **R**, and **Q**, the Kalman matrix of gains ($\mathbf{K}_a$) of Eq. (20) is

$$\mathbf{K}_a = \begin{bmatrix} [\mathbf{K}_f] \\ [\mathbf{K}_s] \end{bmatrix} = \begin{bmatrix} \begin{bmatrix} [\mathbf{K}_1] \\ [\mathbf{K}_2] \end{bmatrix} \\ \begin{bmatrix} [\mathbf{K}_3] \\ \vdots \\ [\mathbf{K}_{2n+2}] \end{bmatrix} \end{bmatrix}. \tag{22}$$

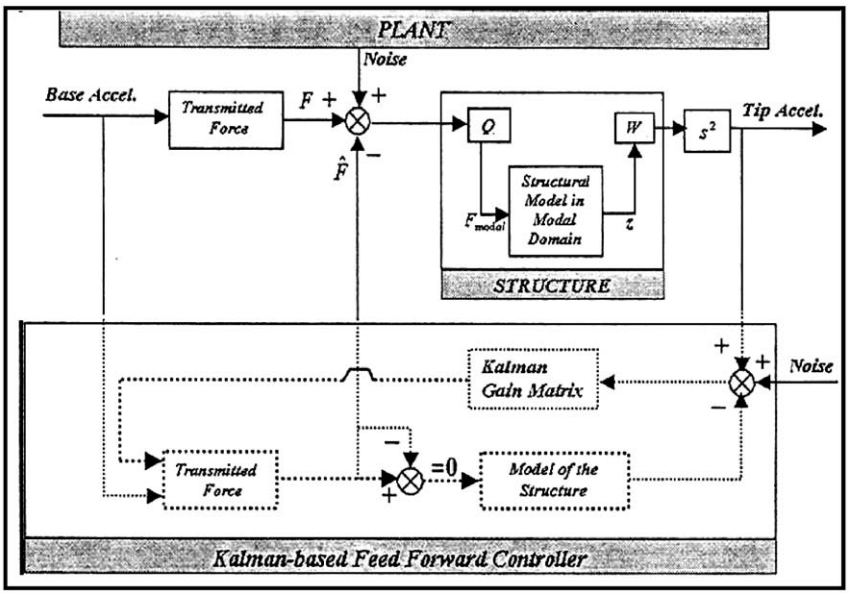

Fig. 3. Schematic of the control strategy.

Eq. (23) shows that $\mathbf{K}_a$ is partitioned into two parts, namely, $\mathbf{K}_f$ which corrects the estimates of $\mathbf{x}_f$ of Eq. (14), and $\mathbf{K}_s$ which corrects the estimates beam states (i.e., $\mathbf{X}_t$ of Eq. (15)).

In general, the dynamics of the Kalman estimator takes on a particularly simple structure that closely resembles the original dynamic system to be controlled [15,16]. The complete vibration isolation scheme proposed by this study is shown in Fig. 3.

It is well known that the Kalman estimator should be subject to all the deterministic inputs the plant is subject to, including the estimated control Force $\hat{\mathbf{F}}$ shown in Fig. 3. This is why the realization of the structure inside the controller in Fig. 3 is subject to the estimated transmitted force ($\hat{\mathbf{F}}$) twice. These two forces have the same magnitude, and like the two forces acting on the structure (plant), they are opposite in sign, zeroing the net force seen by the realization of the structure inside the controller. Therefore, the Kalman estimate of the acceleration, of any point on the beam, is identically zero, which eliminates the need for realizing (including) the structure inside the controller, which subsequently yields a second order control scheme regardless of the order of the plant model. This reduces the computational burden on the controller and lowers its complexity.

4. Numerical simulation and results

The proposed (KAFB) strategy is used in simulating the isolation of the tip of a beam mounted on a vibrating elastic base as shown in Fig. 4. The beam-base system has the dimensions and properties listed in Table 1.

The state-space model of Eq. (14) is utilized to mimic the base dynamics, while the state-space model of Eq. (15) is utilized to mimic the actual dynamic behavior of the beam. The base

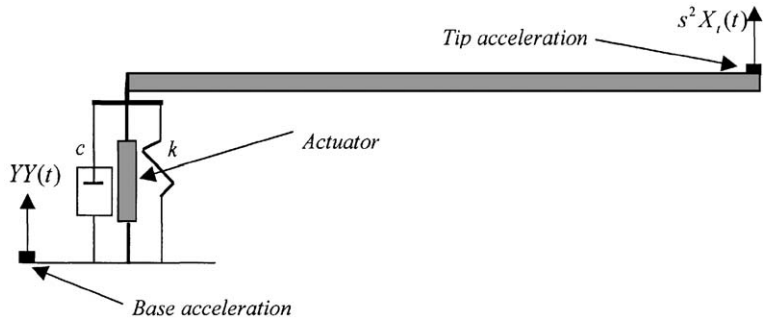

Fig. 4. Control of a cantilevered beam mounted on a vibrating elastic base.

Table 1
Beam-base data

Beam's material properties	Modulus of elasticity $E = 207$ GPa
	Density $\rho = 7800$ kg/m^3
Beam dimensions	Length = 1 m
	Width = 0.05 m
	Thickness = 0.007 m
Elastic base properties	Stiffness $k = 10\,000$ N/m
	Damping $c = 0.01$ kg/s

Table 2
Simulation data used with Matlab® and Simulink®

Base excitation (square wave)	45 Hz with $2g$ amplitude
	150 Hz with $3g$ amplitude
	250 Hz with $3g$ amplitude
	500 Hz with $5g$ amplitude
Measurement noise	Band-limited white noise with 0.01 power and sample time of 0.0001 s
Process noise covariance/measurement noise covariance	$Q/R = 6$ for all excitations

acceleration is simulated by a square wave with various amplitudes and frequencies as listed in Table 2. The acceleration of the beam tip is obtained by differentiating the tip displacement (i.e., $\mathbf{X}_t$ of Eq. (15)) twice.

The reduced-order linear elastodynamic model of the beam-base system, i.e., (plant) needed for construction of the KAFB and the associated Kalman matrix of gains ($\mathbf{K}_a$) is generated according to the procedure given in Eqs. (16)–(22). FE modal analysis of a solid model of the beam discretized by 96-4 node, 0.007 m-thick shell elements, is used to generate the natural frequencies and mode shapes of the beam-base system. The assumed actual behavior of the beam is constructed from the first eight (8) modes of vibration of the beam, while the reduced-order state-space model of the plant (used in constructing KAFB) is constructed from the first three modes of vibration. The natural frequencies of the first eight modes of vibration found by FE modal analysis of the beam are listed in Table 3.

Table 3
Modal frequencies of the beam generated by ANSYS

Mode	1st	2nd	3rd	4th	5th	6th	7th	8th
Freq. (Hz)	36.641	100.62	197.06	259.46	326.20	431.85	488.94	686.39

Modal damping of 1% is added to the system (approximate natural damping of the beam's material), and the damping matrix **C** of Eq. (1) is constructed based on the initial assumption that **C** is proportional to the mass and stiffness matrices **M**, and **K**, respectively. Using the aforementioned data and assumptions, the Kalman matrix of gains ($\mathbf{K}_a$) for this study is

$$\mathbf{K}_a = \begin{bmatrix} [\mathbf{K}_f] \\ [\mathbf{K}_s] \end{bmatrix} = \begin{bmatrix} \begin{bmatrix} 0.01756355385953 \\ -0.00000076074449 \end{bmatrix} \\ \begin{bmatrix} 0.01756355385953 \\ -0.00000076074449 \\ -0.00070438539801 \\ -0.00005360989462 \\ -0.00000954747742 \\ -0.00000004835226 \\ 0.00000000098030 \\ 0.00000000027617 \end{bmatrix} \end{bmatrix}. \tag{23}$$

While the data listed in Table 1 is assumed to be that of the actual system, a high modelling error of 50% is assumed for the flexible beam. This modelling error is incorporated into the simulation by multiplying the matrix ($\mathbf{A}_s$) of Eq. (15) by (1.5). Measurement noise is simulated by a band-limited white noise introduced at the feedback path; see Fig. 3. Simulation data used in this study is listed in Table 2.

The control scheme depicted by Fig. 3 is implemented for the purpose of isolating the beam tip from the vibration of the base in the vertical direction. The isolation mechanism is achieved through counteracting the transmitted force by the actuator force (i.e., $\hat{\mathbf{F}}$), the magnitude and direction of which are calculated by the controller as shown in Fig. 3. A sample plot of the force transmitted to the structure through its elastic base is shown in Fig. 5. Acceleration of the base is the simulated by square wave acting at the point where the actuator is attached to the base. The tip acceleration is taken as the output displacement differentiated twice.

The simulation is carried out using Matlab® and Simulink® where the system is excited by the base excitation signals listed in Table 2, and the acceleration of the beam's tip with and without control is plotted. Tip acceleration (s^2X_t) plots in Figs. 6–10 show that the proposed control method has succeeded in reducing the vibration of the beam tip by roughly 40–60% using only a second order controller. It is also clear that controller has maintained stability and robustness despite the presence of process and measurement noise and near-resonance base excitation conditions.

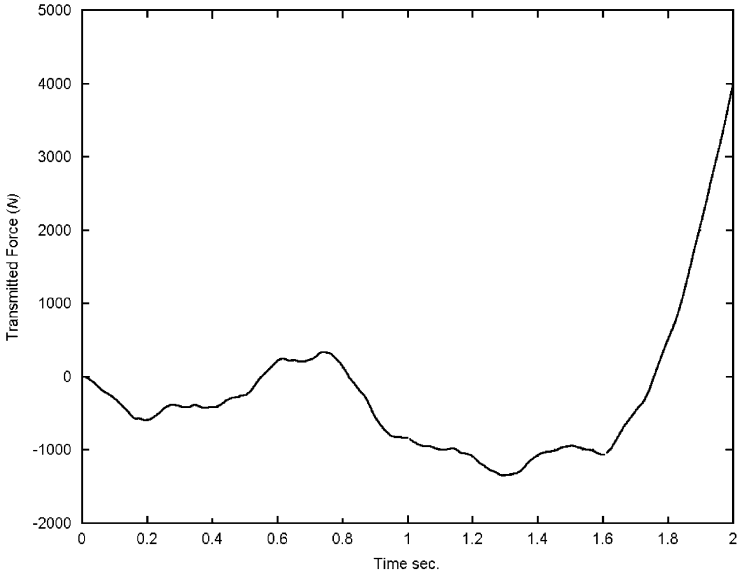

Fig. 5. Sample plot of the force transmitted through elastic base to the structure.

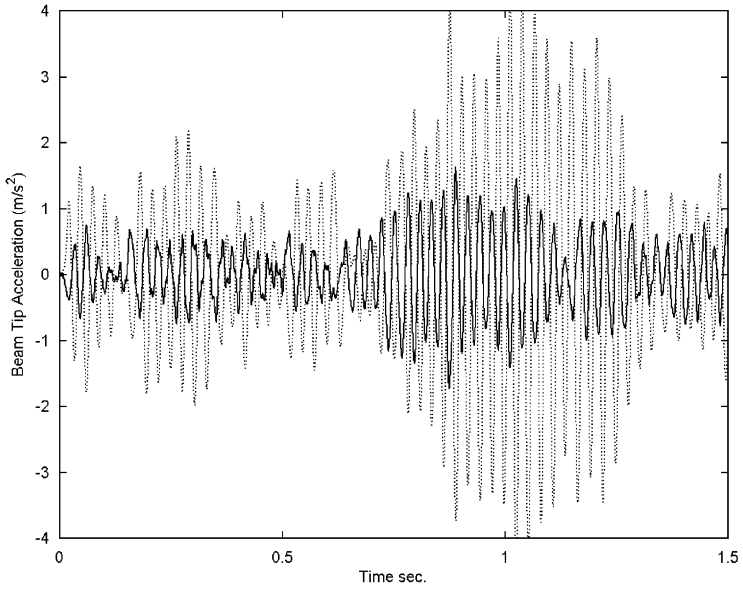

Fig. 6. Tip acceleration with and without control; 12 Hz square wave base excitation with 20 m/s^2 amplitude. No control, ⋯⋯; feedforward–feedback control, ——.

Fig. 3 shows that by disconnecting the feedback signal, the controller becomes a feedforward controller. Such controller will perform well only if (a) the model is highly accurate, (b) the overall controller gain matches the feedforward gain exactly, and (c) the controller path is 180° out of

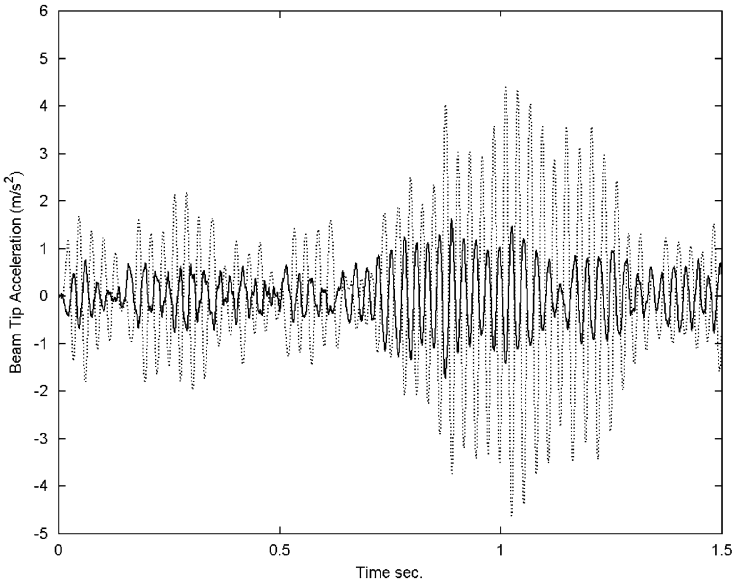

Fig. 7. Tip acceleration with and without control; 150 Hz square wave base excitation with 30 m/s^2 amplitude. No control, ……; feedforward–feedback control, ——.

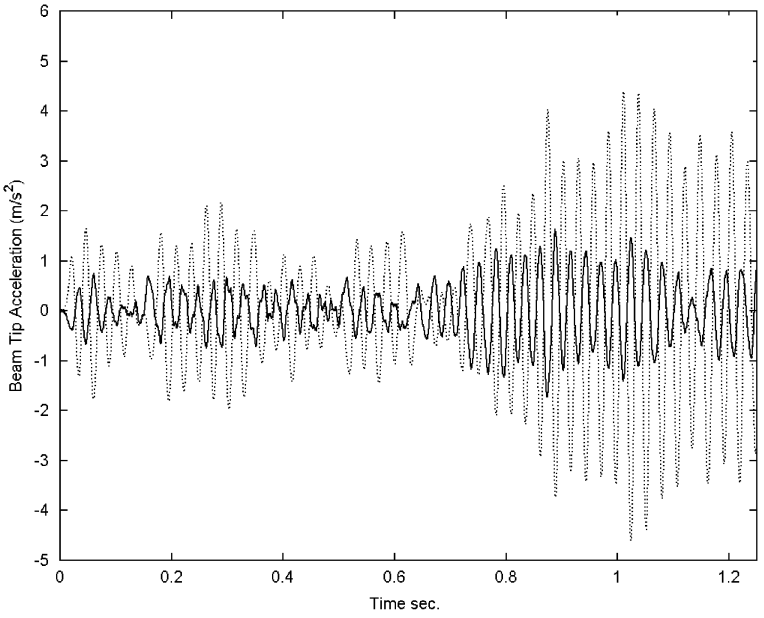

Fig. 8. Tip acceleration with and without control; 250 Hz square wave base excitation with 30 m/s^2 amplitude. No control, ……; feedforward–feedback control, ——.

phase with the feedforward path. If these conditions are not exactly met, the cancellation of the transmitted force will be less effective or, in severe cases of phase mismatch, the controller might actually worsen the system disturbance response.

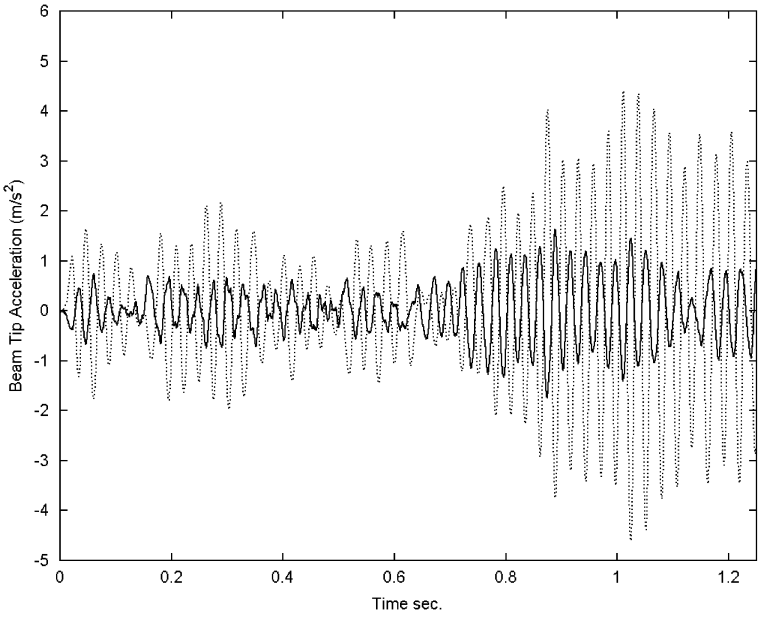

Fig. 9. Tip acceleration with and without control; 500 Hz square wave base excitation with 50 m/s^2 amplitude. No control, ⋯⋯; feedforward–feedback control, ——.

To examine the effect of the feedback signal on the overall controller performance, the process is simulated with the feedback signal disconnected. Comparison between the performance of feedforward only controller, and that of the feedforward–feedback is depicted in Fig. 10 which shows that the active feedforward–feedback controller is more effective than the feedforward only controller where the latter has kept track of the output and constantly adjusted the control effort for optimal vibration isolation at the sensor location (beam tip).

5. Conclusions

This paper describes the design and simulation of a new active feedforward–feedback Kalman estimator-based control strategy (KAFB) using non-collocated actuators and sensors for vibration isolation of flexible structures mounted on a vibrating elastic base. The control strategy developed in this paper focuses on lowering the force transmitted to the structure through its vibrating elastic foundation in the presence of process and measurement noise. A state-space model of the structure is constructed from the natural frequencies and mode shapes generated via FE modal analysis of the base-structure system. An important aspect of the proposed control strategy is that, while it is designed based on a full order model of the physical structure, its implementation is reduced to the realization of a second order estimator regardless of the order of the plant model, and with minimal effect on its accuracy and performance.

Knowing that the dynamics of the Kalman estimator are second order and always resembles the actual system, the speed and agility required for compensating for any phase or magnitude mismatch between the transmitted force and the control force are almost instant. Such high

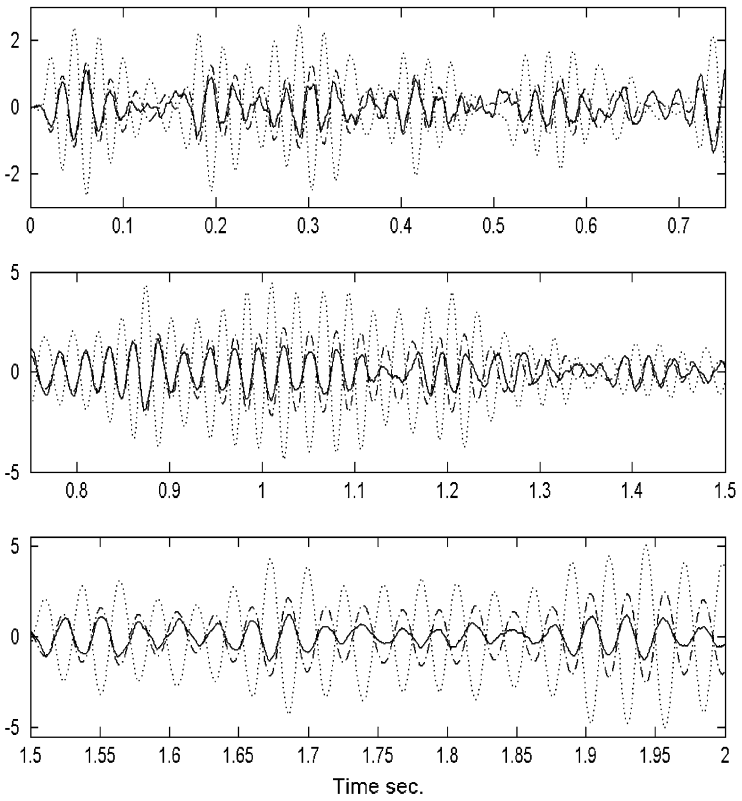

Fig. 10. Tip acceleration with no control, active feedforward control, and active feedforward–feedback control. (A) 0–0.75 s period, (B) 0.75–1.5 s period, and (C) 1.5–2.0 s period. No control, ⋯⋯; feedforward–feedback control, ——; feedforward control, _____.

performance is accredited to the fact that, in addition to being a low order controller and, unlike feedforward controllers, the feedforward–feedback approach also keeps track of the output of the system, where any output deviation from the expected value (zero acceleration) at the sensor location is compensated for by adjusting the magnitude and phase of the control force to achieve the desired zero acceleration at the sensor location.

One added benefit of the proposed control strategy is its digital implementation capabilities due to the fact that the discrete Kalman estimator is exact. Numerical evaluation of the control strategy suggests that it possesses high performance in terms of isolating any location on the structure from the vibration of the structure's elastic base, as well as its considerable robustness in the presence of process and measurement noise. Comparison between active feedforward only and active feedforward–feedback arrangements shows that the latter is more effective in isolating the structure from the vibrating base as shown in Fig. 10. Depending on the nature of the model, measurements, and method of discretization, different noise characteristics arise such that fine tuning of the Kalman filter is need. Fine tuning of the filter is available through variation of the values of $\mathbf{Q}$, and $\mathbf{R}$ until satisfactory values of Eq. (22) are obtained [14,16].

It is worth mentioning that although the model used in the simulation is a relatively low-order one ($n = 8$) the proposed strategy can function equally well for larger models

where the construction of the state-space model of the system using FE modal analysis will be truly needed.

Like other control techniques, the proposed method is not without limitations. One of the limitations of the proposed method is that it is designed to target the isolation of a point or group of points (i.e., sensor(s) locations(s)) on the structure but not the whole structure.

Acknowledgements

The author would like to thank King Fahd University of Petroleum and Minerals for their continuous support.

References

[1] S.J. Elliot, M. Serrand, P. Gardonio, Feedback stability limits for active isolation systems with reactive and inertial actuators, *Journal of Vibration and Acoustics* 123 (2001) 250–261.
[2] B.R. Mace, Active control of flexural vibration, *Journal of Sound and Vibration* 114 (2) (1987) 253–270.
[3] A. El-Sinawi, A.R. Kashani, Active control of engine mounts, Society of Automotive Engineers, paper no. 1999-01-1845, 1999.
[4] C.M. Harris, C.E. Crede, *Shock and Vibration Handbook*, McGraw-Hill, New York, 1976, 30-1–32-1.
[5] F. Wallace, Understanding hydraulic mounts for improved noise, vibration, and ride quality, Society of Automotive Engineers, Technical Report No. 850975, 1985.
[6] C.E. Kaplow, C.E. Velman Jr., Active local vibration isolation applied to a flexible space telescope, *AIAA Journal of Guidance and Control* 3 (1998) 227–233.
[7] P. Gardonio, S.J. Elliot, R.J. Pinnington, Active isolation of structural vibration on a multiple-degree-of-freedom system, Part I: the dynamics of the system, *Journal of Sound and Vibration* 207 (1) (1997) 61–93.
[8] P. Gardonio, S.J. Elliot, R.J. Pinnington, Active isolation of structural vibration on a multiple-degree-of-freedom system, Part II: effectiveness of the active control strategies, *Journal of Sound and Vibration* 207 (1) (1997) 61–93.
[9] J.R. Clover, Adaptive noise cancellation applied to sinusoidal interference, *IEEE Transaction on Acoustics, Speech, and Signal Processing* 25 (6) (1979) 484–491.
[10] S.M. Kuo, D. Vijayan, Adaptive algorithm and experimental verification of feedback active noise control, *Noise Control Engineering Journal* 42 (2) (1994) 37–46.
[11] A. Yousefi-Koma, G. Vukovich, Vibration suppression of flexible beams with bounded piezo-transducers using wave absorbing controllers, *Journal of Guidance, Control and Dynamics* 23 (20) (2000) 347–354.
[12] W. Gawronski, T. Williams, Modal reduction for flexible space structures, *Journal of Guidance* 4 (10) (1991) 68–76.
[13] A. El-Sinawi, Vibration Suppression in Machining using a Kalman Estimator-based Controller, Ph.D. Dissertation, University of Dayton, Dayton, OH, 1999.
[14] F. Lewis, *Optimal Control*, Wiley, Cambridge, MA, 1986.
[15] R.E. Kalman, R.S. Bucy, New results in linear filtering and prediction theory, *Journal of Basic Engineering* 1 (1961) 95–101.
[16] B. Hassibi, A.H. Sayed, T. Kailath, *Indefinite-Quadratic Estimation and Control*, SIAM Publication, Philadelphia, 1999.